A MESOSCALE AIR-ICE-OCEAN FEEDBACK MECHANISM FOR THE ICE DRIFT IN THE MARGINAL ICE ZONE

P. C. Chu
Department of Oceanography
Naval Postgraduate School
Monterey, California

ABSTRACT

Ice drift in the marginal ice zone (MIZ) is a very important feature of air-ice-ocean interaction at high latitude. Thermally generated surface winds, blowing from ice to water (ice breeze) with some deflection due to the earth rotation, force the ice drift and ocean currents near the MIZ. By changing the surface temperature gradient, the ice motion and the ocean currents feed back on the surface winds. A coupled air-ice-ocean theoretical model for the MIZ is employed to discuss the ice drift pattern with such a feedback mechanism. The steady-state solutions show that an off-ice and divergent wind field not only produces a dilation of the MIZ (as people generally think), but also generates a compaction of MIZ for some circumstances. An ice divergence/convergence criterion is found. The time-dependent solutions show that the ice motion exhibits two bifurcations. First, it bifurcates into decaying and growing modes. Second, the growing mode bifurcates into non-oscillatory and oscillatory states. Finally, the model predicts the ice edge upwelling.

NOMENCLATURE

A	ice concentration
a_{kj}	integral constant
b_k	integral constant
C_{ai}	air drag coefficient on ice, 0.0036
C_{aw}	air drag coefficient on water, 0.0012
C_{wi}	water drag coefficient on ice, 0.00086 m/s
DT_0	mean surface temperature difference across the MIZ
g	gravitational acceleration, $9.81 m/s^2$
g^*	reduced gravitational acceleration, $0.005 m/s^2$
H_i	mean ice thickness
H_w	equilibrium depth of the pycnocline
h_w	thickness of the upper ocean
k	wave number
L	length scale twice the MIZ width, 200 km
R	rate for Rayleigh friction and Newtonian cooling, $2.08 \times 10^{-5}/s$
Ri	atmospheric Richardson number
U	scale of ice breeze wind
u_a, v_a	ice breeze wind
u_i, v_i	ice drift velocity
u_w, v_w	ocean cuurent
α	angle between surface wind and surface temperature gradient
β	angle between ice velocity and surface wind
δ	thickness of atmospheric Ekman layer
ζ	nondimensional ice edge displacement
θ_a	surface temperature
θ_{a0}	characteristic surface temperature, $270^\circ K$
λ_{kj}	eigenvalue for vertical structure
μ_k	eigenvalue for time evolution
ν	air vertical eddy viscosity, $5\ m^2/s$
ρ_a	air density, $1.29\ kg/m^3$
ρ_i	ice density, $920\ kg/m^3$
ρ_w	water density, $1000\ kg/m^3$
Ω	angular velocity of the Earth rotation, $0.7292 \times 10^{-4}/s$.

INTRODUCTION

The importance of ice breeze in the MIZ is discussed as follows. Schmidt (1947) used a simple linear model to depict seabreeze/landbreeze phenomena and concluded that for a maximum land-water temperature gradient of $4.3^\circ K/100km$, a maximum landbreeze intensity of about 2 m/s would be reached. From observations in the Southern Bering Sea, Reynolds et al. (1985) estimated that ice floes drift to the right of the wind by approximately 30° at about 4% of the wind speed at 3m. The ice breeze is analogous to the landbreeze. Therefore, $1^\circ K/100km$ surface temperature gradient roughly produces 0.5 m/s ice breeze, which in

Presented at the Seventh International Conference on Offshore Mechanics and Arctic Engineering
Houston, Texas — February 7-12, 1988

Report Documentation Page

Form Approved
OMB No. 0704-0188

1. REPORT DATE	2. REPORT TYPE	3. DATES COVERED
1988		**00-00-1988 to 00-00-1988**

4. TITLE AND SUBTITLE	5a. CONTRACT NUMBER
A Mesoscale Air-Ice-Ocean Feedback Mechanism for the Ice Drift in the Marginal Ice Zone	5b. GRANT NUMBER
	5c. PROGRAM ELEMENT NUMBER
6. AUTHOR(S)	5d. PROJECT NUMBER
	5e. TASK NUMBER
	5f. WORK UNIT NUMBER
7. PERFORMING ORGANIZATION NAME(S) AND ADDRESS(ES) **Naval Postgraduate School,Department of Oceanography,Monterey,CA,93943**	8. PERFORMING ORGANIZATION REPORT NUMBER
9. SPONSORING/MONITORING AGENCY NAME(S) AND ADDRESS(ES)	10. SPONSOR/MONITOR'S ACRONYM(S)
	11. SPONSOR/MONITOR'S REPORT NUMBER(S)

12. DISTRIBUTION/AVAILABILITY STATEMENT
Approved for public release; distribution unlimited

13. SUPPLEMENTARY NOTES
Offshore Mechanics and Arctic Engineering, 4, 83-90

14. ABSTRACT
see report

15. SUBJECT TERMS

16. SECURITY CLASSIFICATION OF:			17. LIMITATION OF ABSTRACT	18. NUMBER OF PAGES	19a. NAME OF RESPONSIBLE PERSON
a. REPORT **unclassified**	b. ABSTRACT **unclassified**	c. THIS PAGE **unclassified**	**Same as Report (SAR)**	**8**	

turn generates about 2 cm/s ice flow. Paquette and Bourke (1979), during a summer cruise in the Chukchi Sea, found the sea surface temperature to change by over 6°K across a distance of about 25 km as the ice concentration fell from seven-eighths cover to zero. This is an enormous gradient by most oceanic standards (McPhee, 1983). Under such a condition it is found that the ice breeze is around 12 m/s (Schmidt 's estimation), and the associated ice drift is about 48 cm/s (Reynold et al 's estimation). The coupled air-ice-ocean model contains three parts: a thermally forced boundary layer air flow, a mechanically driven ice drift, and a reduced gravity ocean. The three components are linked through the surface temperature gradient and various interfacial stresses.

THERMALLY FORCED BOUNDARY LAYER AIR FLOW

A K-theory approach planetary boundary layer air model with modified Boussinesq approximation and with constant stress sublayer treated by Kuo (1973) and Chu (1986, 1987a,b,c) is employed to compute surface wind (ice breeze) thermally driven by surface temperature gradient across the ice edge. The x-axis is in the cross ice-edge direction (positive iceward), and the y-axis is parallel to the ice edge, as shown in Fig.1. It is considered that spatial variations in the MIZ are much large perpendicular to the ice edge than parallel to it, and hence derivatives with respect to y are assumed to be zero. As discussed by Chu (1986) the waterward/iceward migration of the MIZ increases/decreases the surface temperature gradient. The effects of ice flow on the surface temperature gradient can be depicted by (Chu, 1987b)

$$\partial^2\theta_a/\partial t\partial x = (\pi DT_0/L^2)u_i(x,t) \qquad (1)$$

where θ_a is a surface temperature, u_i is an ice drift velocity in the cross ice-edge direction, DT_0 is a characteristic surface temperature differnce across the MIZ, and L is a length-scale twice the MIZ width. Subscripts 'a' and 'i' denote atmosphere and ice, respectively. The surface temperature is separated into a steady state and a time-dependent part. Both parts are decomposed into Fourier sine series. The fact that the waterward monotonically increasing surface temperature often observed near the MIZ (Muench, 1983) implies that the steady state only has the first mode, i.e.,

$$\theta_a(x,t)=\sum_K \theta_{ak}(t)\sin k\pi x/L + \theta_a \sin \pi x/L \qquad (2)$$

where θ_{ak} and θ_a are Fourier coefficients. Integrating Kuo's (1973) planetary boundary layer model with slip and kinematic boundary conditions at the surface and finite condition at the top, the thermally driven surface wind is given by (Chu, 1986, 1987a,b,c)

$$u_a(x,t)=\sum_K u_{ak}\tau_{ik}(t)\cos k\pi x/L + u_{a1}\cos \pi x/L \qquad (3)$$

$$v_a(x,t)=\sum_K v_{ak}\tau_{ik}(t)\cos k\pi x/L + v_{a1}\cos \pi x/L \qquad (4)$$

where (u_a,v_a) is a surface wind vector, and u_{ak} and v_{ak} are constants defined by

$$u_{ak} \equiv U\sum_{j=1}^{3} a_{kj}\lambda_{kj},$$
$$v_{ak} \equiv U(b_k - 2f_0\sum_{j=1}^{3} a_{kj}/\lambda_{kj}),\ k=1,2,... \qquad (5)$$

where $f_0=\sin\varphi$, φ is the latitude, and

$$U \equiv g\delta DT_0/(2L\Omega\theta_{a0}) \qquad (6)$$

is the scale of ice breeze wind. Here $\delta=(\nu/\Omega)^{1/2}$ is the Ekman depth, ν is the air vertical eddy viscosity, and θ_{a0} is a characteristic air temperature at surface. According to Kuo (1973), ν is taken as 5 m^2/s. The eigenvalues λ_{kj} are the roots with negative real parts of following sixth order algebraic equations:

$$\lambda^6+4f_0^2\lambda^2 - 4k^2\pi^2Ri=0,\ k=1,2,... \qquad (7)$$

where

$$Ri \equiv (\delta N/2L\Omega)^2 \qquad (8)$$

is the air Richardson number. N is the air Brunt-Vaisaila frequency. The integral constants a_{kj} and b_k in (5) are the roots of the following nonhomogeneous linear algebraic equations

$$\sum_{j=1}^{3} a_{kj} = 0,$$
$$\sum_{j=1}^{3} \lambda_{kj}(1 - M\lambda_{kj})\, a_{kj} = 0,$$
$$-2f_0 \sum_{j=1}^{3} (a_{kj}/\lambda_{kj})(1-M\lambda_{kj}) + b_k = 0,$$
$$2k\pi Ri \sum_{j=1}^{3} a_{kj}/\lambda_{kj}^2 = -1/k. \qquad (9)$$

where M is a measure of the effective depth of the constant stress-sublayer (Kuo, 1973): $M=\nu/(C_{ai}U\delta)$, here C_{ai} is an air drag coeffient on ice. The ice-ocean system is mechanically driven by the surface wind, therefore, ice velocity should have the same Fourier components as the wind, i.e.,

$$u_i(x,t)=\sum_K u_{ik}(t)\cos k\pi x/L + u_i\cos \pi x/L \qquad (10)$$

$$v_i(x,t)=\sum_K v_{ik}(t)\cos k\pi x/L + v_i\cos \pi x/L \qquad (11)$$

where (u_i,v_i) is the ice velocity vector, u_{ik}, v_{ik}, u_i, and v_i are Fourier coefficients. $\tau_{ik}(t)$ in (3)-(4) is defined as nondimensional ice edge displacement (Chu, 1986, 1987b), i.e.,

$$Ld\tau_{ik}/dt = u_{ik}(t) \qquad (12)$$

If f_0 (i.e., Latitude), Ri, and M are known, the eigenvalues λ_{kj} and the integral constants a_{kj} and b_k are easily obtained by solving the algebraic equations (7) and (9).

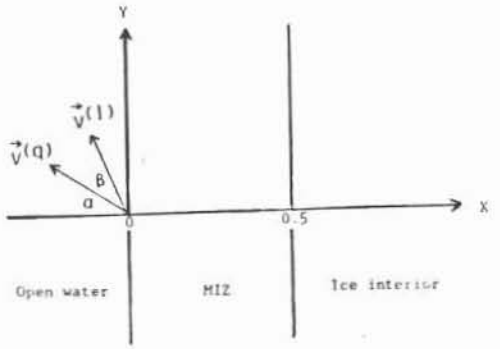

Fig. 1. The coordinate system and air deflection angle α, ice turning angle β

FREE ICE DRIFT MODEL

Roed and O'Brien (1983) showed that the internal ice stress and the nonlinear terms aren't crucial for the MIZ dynamics, therefore, the ice is nearly free drift. The momentum equations of the ice drift are given by

$$\partial u_i/\partial t - fv_i = \gamma_{ai}u_a + \gamma_{wi}(u_w-u_i) \quad (13)$$

$$\partial v_i/\partial t + fu_i = \gamma_{ai}v_a + \gamma_{wi}(v_w-v_i) \quad (14)$$

where the terms on the right-hand side represent the water and air stresses on ice, respectively. Here

$$\gamma_{ai} \equiv \rho_a C_{ai} U/(\rho_i H_i), \quad \gamma_{wi} \equiv \rho_w C_{wi}/(\rho_i H_i) \quad (15)$$

C_{wi} is a dimensional (m/s) water drag coefficient on ice (Reod and O'Brien, 1983), and ρ_a, ρ_i, and ρ_w are the densities of air, ice, and water, respectively. H_i is a mean ice thickness.

REDUCED GRAVITY OCEAN MODEL

Suppose that the ocean is composed of two layers, in which the lower layer is deep enough for motion in the lower layer to be vanishingly small. Such a model is referred to as a reduced gravity model. Furthermore, the model has the simplest form of dissipation, namely, Rayleigh friction with decay rate R and Newtonian cooling, also with decay rate R. The momentum and continuity equations for the ocean are written by (Gill, 1982; Roed and O'Brien, 1983)

$$(\partial/\partial t+R)u_w - fv_w = -g^*\partial h_w/\partial x + (1-A)\gamma_{aw}u_a + A\gamma_{iw}(u_i-u_w) \quad (16)$$

$$(\partial/\partial t+R)v_w + fu_w = (1-A)\gamma_{aw}v_a + A\gamma_{iw}(v_i-v_w) \quad (17)$$

$$(\partial/\partial t+R)h_w + H_w\partial u_w/\partial x = 0 \quad (18)$$

where the second and third terms on the right-hand side of (16) and (17) represent the air and ice stresses on water, and g* is a reduced gravitational acceleration. H_w the equilibrium depth of the pycnocline, h_w the thickness of the upper layer, $\gamma_{iw} \equiv C_{wi}/H_w$, and $\gamma_{aw} \equiv \rho_a C_{aw} U/\rho_w H_w$, C_{aw} is an air drag coefficient on water. A is the ice compactness or ice concentration (i.e., the fraction of area covered by ice). Hibler and Ackley (1983) took the 50% limit of A as the ice edge. Inside the MIZ, the ice concentration, A, decreases waterward very slowly from the boundary between pack ice and the MIZ (where A~1) to some place near the ice edge, and then diminishes very rapidly to the ice edge. If the area we focus on is not very close to the ice edge, we may set A~1. The portion of air stress on the water, $(1-A)\gamma_{aw}V_a$, is then neglected compared to ice stress on the water, $A\gamma_{iw}(V_i-V_w)$. Setting A=1 and eliminating h_w from (16) and (18), the momentum equations (16) and (17) become

$$(\partial/\partial t+R)u_w - fv_w - (g^*H_w/RL^2)\partial^2 u_w/\partial x^2 = \gamma_{iw}(u_i-u_w) \quad (19)$$

$$(\partial/\partial t+R)v_w + fu_w = \gamma_{iw}(v_i-v_w) \quad (20)$$

SOLUTIONS

If the ice-ocean is considered as one system, the air stress is the only forcing term in (13), (14), (19), and (20). The ice velocity and the ocean current should have the same Fourier components as the surface wind since our system is linear. According to (3) and (4) the solutions have the following forms:

$$u_i(x,t) = \sum_k u_{ik}\exp(\mu_k t)\cos k\pi x/L + \bar{u}_i\cos\pi x/L \quad (21a)$$

$$v_i(x,t) = \sum_k v_{ik}\exp(\mu_k t)\cos k\pi x/L + \bar{v}_i\cos\pi x/L \quad (21b)$$

$$u_w(x,t) = \sum_k u_{wk}\exp(\mu_k t)\cos k\pi x/L + \bar{u}_w\cos\pi x/L \quad (21c)$$

$$v_w(x,t) = \sum_k v_{wk}\exp(\mu_k t)\cos k\pi x/L + \bar{v}_w\cos\pi x/L \quad (21d)$$

where u_{ik}, v_{ik}, u_{wk}, v_{wk} (k=1,2,...), $\bar{u}_i$, $\bar{v}_i$, $\bar{u}_w$, and $\bar{v}_w$ are the Fourier coeffients, and μ_k (k=1,2,...) are the eigenvalues of the system. Substituting (21a)-(21d) into (13), (14), (19), and (20) we have a set of nonhomogeneous linear algebraic equations for the steady-state Fourier coefficients ($\bar{u}_w$, $\bar{v}_w$, $\bar{u}_i$, and $\bar{v}_i$):

$$[R+\pi^2 g^*/(RL^2)+C_{iw}]\bar{u}_w - f\bar{v}_w - \gamma_{iw}\bar{u}_i = 0, \quad (22a)$$

$$f\bar{u}_w + (R+C_{iw})\bar{v}_w - \gamma_{iw}\bar{v}_i = 0, \quad (22b)$$

$$-\gamma_{wi}\bar{u}_w + \gamma_{wi}\bar{u}_i - f\bar{v}_i = \gamma_{ai}\bar{u}_{a1} \quad (22c)$$

$$-\gamma_{wi}\bar{v}_w + \gamma_{wi}\bar{v}_i + f\bar{u}_i = \gamma_{ai}\bar{v}_{a1} \quad (22d)$$

and the dispersion relations for the eigenvalues μ_k:

$$\begin{vmatrix} \mu_k+\gamma_{wi} & -f & \gamma_{ai}u_{ak}/L & \gamma_{wi} & 0 \\ f & \mu_k+\gamma_{wi} & \gamma_{ai}v_{ak}/L & 0 & \gamma_{wi} \\ 1 & 0 & \mu_k & 0 & 0 \\ \gamma_{iw} & 0 & 0 & \mu_k+R_1 & -f \\ 0 & \gamma_{iw} & 0 & f & \mu_k+R_0 \end{vmatrix} = 0, \quad (23)$$

where $R_0 = R+C_{iw}$, $R_1 = R_0 + g^*H_w\pi^2k^2/RL^2$.

MEAN ICE DIVERGENCE/CONVERGENCE CRITERION

In this section we discuss the steady state solutions (22a)-(22d). Chu (1987c) shows that the absolute value of ice breeze deflection angle (angle between surface temperature gradient and surface wind), $|\alpha|$, increases with increasing latitude and decreases with increasing Ri. At 65° (N and S) latitude it varies from 41.8° when Ri = 0.001 to α = 27.5° when Ri = 0.04. The angle between surface wind and ice velocity, β (as shown in Fig.2), is defined by

$$\beta = \tan^{-1}(\bar{v}_i/\bar{u}_i) - \alpha \qquad (24)$$

where u_i and v_i are the roots of linear algebraic equations (22a)-(22d). An ice divergence/convergence criterion is simply

$$|\alpha+\beta| \begin{cases} > \pi/2 & \text{ice convergence} \\ \\ < \pi/2 & \text{ice divergence} \end{cases} \qquad (25)$$

Fig.2 indicates the mean ice divergence/convergence criterion,

$$\tan^{-1}(\bar{v}_i/\bar{u}_i) = \pi/2 \qquad (26)$$

for different Ri in the (H_i,H_w) plane. The curves separate the parameter plane (H_i,H_w) into ice convergence and ice divergence parts. We can differentiate between ice divergence and ice convergence due to the ice breeze in the MIZ by the parameters Ri, H_i, and H_w. Ice divergence appears in the small H_i and large H_w area, however on the contrary, ice convergence appears in the large H_i and small H_w region. The critical curve ($|\alpha+\beta|=\pi/2$) moves from lower left to upper right in the (H_i,H_w) plane from less to more stable atmosphere. If the drag coefficient C_{wi} is doubled, the turning angle β only has minor changes (less than 10%).

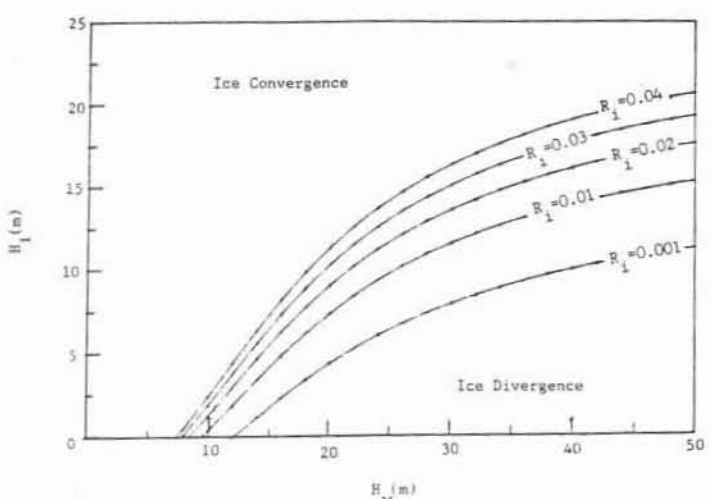

Fig.2. H_i-H_w curves for zero ice divergence/convergence for five different values of Ri (after Chu, 1987a).

TWO BIFURCATIONS OF TIME-DEPENDENT ICE DRIFT

Ice drift observations in the Greenland Sea from 1978 April 28 to September 3 (Vinje, 1982) show two different types of ice motion: oscillatory and nonoscillatory. The mesoscale air-ice-ocean feedback mechanism may explain this phenomena. If the ocean is deep enough such that C_{iw} can be neglected against R, the dispersion relation (23) is simplified as

$$\begin{vmatrix} \mu_k+R+\pi^2k^2g^*H_w/RL^2 & -f \\ f & \mu_k+R \end{vmatrix} = 0, \qquad (27)$$

representing inertial-gravity water waves, and

$$\begin{vmatrix} \mu_k+C_{wi} & -f & C_{ai}u_{ka}/L \\ f & \mu_k+C_{wi} & C_{ai}v_{ka}/L \\ 1 & 0 & \mu_k \end{vmatrix} = 0 \qquad (28)$$

showing the ice drift patterns. The roots μ_k (k=1,2,...) of the cubic equations (28) give the e-folding time dependence of the kth component of ice velocity. The instability criterion for the kth mode of ice motion in the MIZ can be written

$$\mathrm{Re}(\mu_k) < 0 \qquad (29a)$$

the kth mode of ice velocity decreases with time,

$$\mathrm{Re}(\mu_k) = 0 \qquad (29b)$$

neutral, and

$$\mathrm{Re}(\mu_k) > 0 \qquad (29c)$$

the kth mode of ice velocity increases with time. We define the time-increasing mode of ice velocity as an unstable mode.

The oscillation criterion for the kth mode of ice motion is given by

$$\mathrm{Im}(\mu_k) = 0, \text{ (nonoscillatory)} \qquad (30a)$$

$$\mathrm{Im}(\mu_k) \neq 0, \text{ (oscillatory)} \qquad (30b)$$

We compute all the roots of (28) for different values of the parameters H_i, N, DT_0, and obtain three roots μ_1, μ_2, μ_3 at each point of the parameter space (H_i,N^2, DT_0). Here μ_1 is real throughout that space, and μ_2 and μ_3 are real for some values of (H_i,N^2,DT_0) and are complex else where.

Fig.3 shows the surface μ_1=0 for k=1 in the three dimensional space (H_i,N^2,DT_0). This surface divides the space into two parts corresponding to growing and decaying modes. The growing mode generally appears when DT_0 exceeds some critical value around 10°C. This critical value decreases with H_i, and becomes very small (around 1°C) in the region of small mean ice-thickness H_i (H_i<1.5 m). Ice motion corresponding to the eigenvalue μ_1 is nonoscillatory.

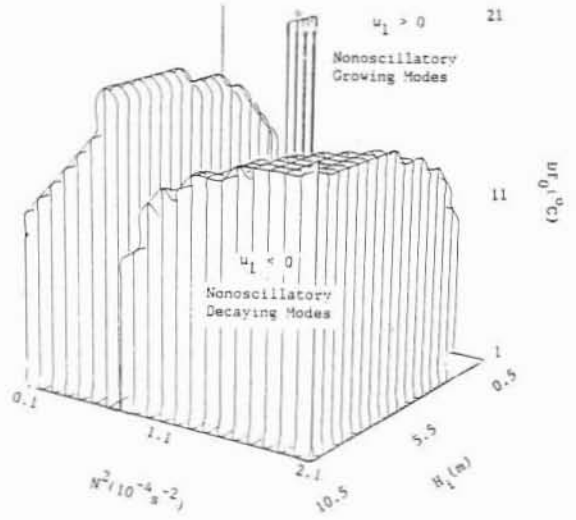

Fig. 3. Separation of nonoscillatory decaying and growing modes referring to real eigenvalues μ_1 for k=1 (after Chu, 1986).

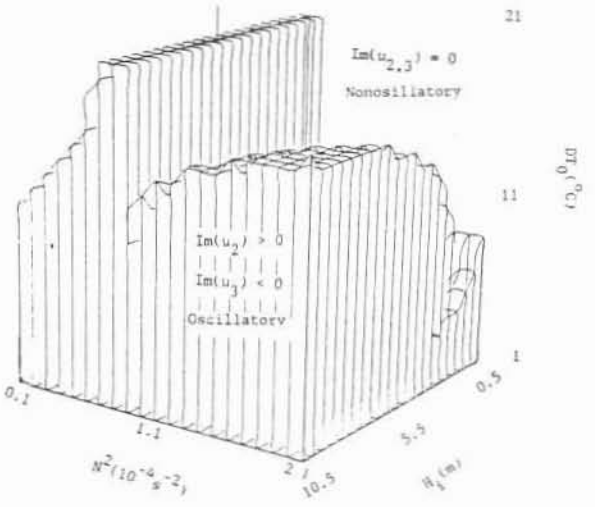

Fig. 5. Separation of nonoscillatory and oscillatory states referring to eigenvalues μ_2 and μ_3 for k=1 (after Chu, 1986).

Fig. 4 indicates the surface of $Re(\mu_2)=0$ (or $Re(\mu_3)=0$) for k=1 in the parameter space (H_1, N^2, DT_0). This surface separates the whole space into growing and decaying parts. The growing mode is present when DT_0 exceeds some critical value which is a function of H_1 and N^2 (when H_1= 4.5 m and N^2=0.00011/s^2, the critical value is 3°C).

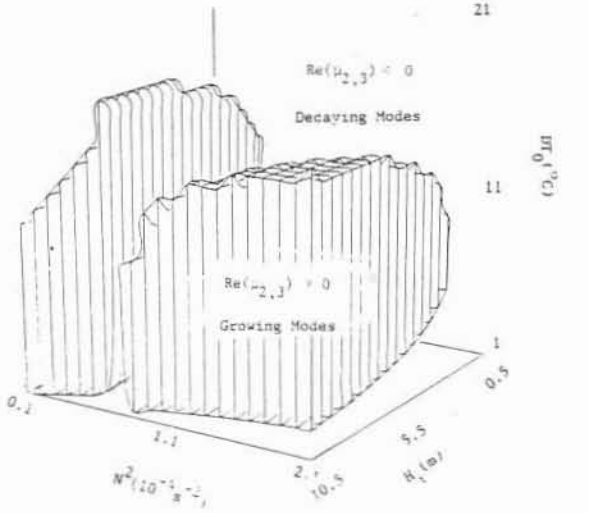

Fig. 4. Separation of decaying and growing modes referring to eigenvalues μ_2 and μ_3.

Fig. 5 reveals the segregation of nonoscillatory and oscillatory modes relating to μ_2 and μ_3. Comparing Fig. 5 with 4, we find that the decaying mode of μ_2 and μ_3 is generally nonoscillatory whereas the growing mode of μ_2 and μ_3 is generally oscillatory.

Fig. 3-5 show the following results: (i) both nonoscillatory and oscillatory modes share a common area (restricted to the region of small DT_0) in the parameter space; however, (ii) nonoscillatory and oscillatory growing modes occupy different regions in the parameter space. The segregation of the two modes depends largely on DT_0 and H_1.

Whether ice motion grows or decays substantially depends on a first critical value of the parameter DT_0 (when $N=1.45\times10^{-2}s^{-2}$ and H_1=2.5m, this critical value is 5°C). When DT_0 is smaller than the first critical value, the motive force is so small that it cannot overcome dissipative effects and does not make ice motion unstable. If DT_0 becomes large enough to overcome the dissipative effects of friction, ice motion becomes larger.

Whether ice motion is oscillatory or nonoscillatory largely depends on DT_0 and the properties of ice. If DT_0 exceeds the first critical value but does not reach a second critical value which mostly depends on N (i.e., when N=0.0145/s, the second critical value is 14°C), and when ice is thin (generally during summer) the ice motion is nonoscillatory, however, when the ice is thick (generally during winter) the ice motion is oscillatory. If DT_0 exceeds the second critical value, only the nonoscillatory growing mode appears.

For the nonoscillatory growing mode the time during which the ice doubles its speed is

$$T_1 = \ln(2/\mu_1), \quad (\mu_1>0) \tag{31}$$

The doubling time treated as a function of DT_0 (for H_1=1m, N=0.01/s) is shown in Fig. 6, which displays a decrease of T_1 with an increase of DT_0. T_1 changes from 2.2 to 0.18 hr as DT_0 varies from 5° to 22°C.

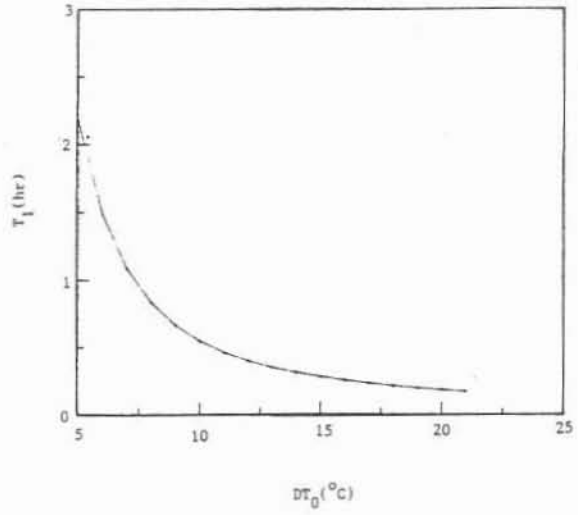

Fig. 6. Dependence of doubling time on DT_0 for the nonoscillatory growing mode for H_i=1m and $N=10^{-4}s^{-1}$ (after Chu, 1986).

The oscillatory growing mode is ice motion due to μ_2 (or μ_3), whose real part is positive and the imaginary part is different from zero. The growing oscillatory mode is located in the area where DT_0 is larger than the first critical value and smaller than the second critical value. As in the nonoscillatory case the growth rate $Re(\mu_{2,3})$ increase with an increase of DT_0 (increase of forcing). The period of the oscillatory mode is defined by

$$T_p = 2\pi/|Im(\mu_{2,3})| \tag{32}$$

Fig. 7 shows the doubling time and the period as a function of DT_0 for H_i=5m and N=0.01/s. The doubling time decreases monotonically with an increase of DT_0. However, the period increases slightly when DT_0 varies from 5°C to 10°C, and then increases rapidly with DT_0. When DT_0 = 12.5°C the period is nearly one day.

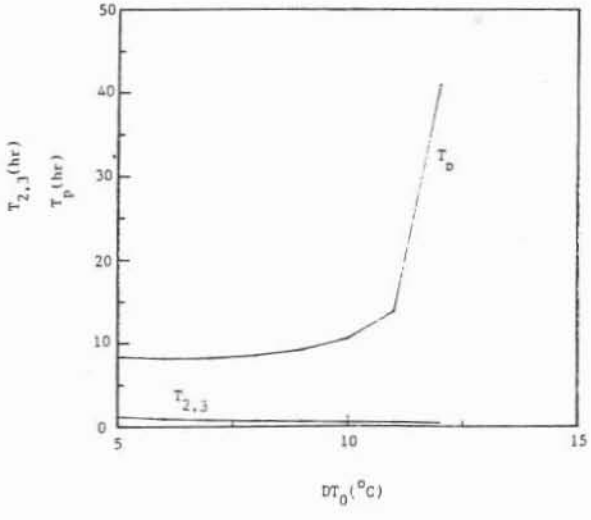

Fig. 7. Dependence of doubling time and period on DT_0 for oscillatory growing mode for H_i=5m and $N=10^{-4}s^{-1}$ (after Chu, 1986).

ICE EDGE UPWELLING

Buckley et al. (1979) reported a pronounced wind-driven upwelling along the edge of the ice pack in an expedition into the Arctic Ocean north of Spitsbergen. The aim of this section is to investigate the effect of the air-ice-ocean feedback mechanism on ice edge upwelling. If the sinusoidal type surface temperature perturbation across the MIZ doesn't change as the ice edge moves in a speed u_i, the parameterization of surface thermal condition (1) becomes

$$\theta_a(x,t)=\theta_{a0} - DT_0 \sin\pi[(x-u_i t)/L] \tag{33}$$

The negative sign in (34) comes from the x-axis pointing iceward (Fig. 1). Let $\xi=(x-u_i t)/L$, the surface wind driven by the horizontal temperature gradient (33) is calculated by

$$u_a|_{z=0} = u_{a1}\cos\pi\xi, \tag{34}$$

$$v_a|_{z=0} = v_{a1}\cos\pi\xi, \tag{35}$$

where u_{a1} and v_{a1} are computed by (5). Neglecting inertial oscillation and assuming the ocean velocities to be small (Roed and O'-Brien, 1983), the momentum equations for the reduced gravity ocean model (19) and (20) are written by

$$Ru_w - fv_w = -g^*\partial h_w/\partial x + [1-H(\xi)]C_{aw}u_{a1}\cos\pi\xi + C_{iw}(u_i-u_w)H(\xi) \tag{36}$$

$$(\partial/\partial t+R)v_w + fu_w = [1-H(\xi)]C_{aw}v_{a1}\cos\pi\xi + C_{iw}(v_i-v_w)H(\xi) \tag{37}$$

where $H(\xi)$ is the Heaviside function defined as

$$H(\xi)\begin{cases} 1, & \text{if } \xi>0, \text{ (MIZ)} \\ 0, & \text{if } \xi<0, \text{ (open water)} \end{cases} \tag{38}$$

The equations for the free drift ice (13), (14) and for the reduced gravity ocean (36), (37), and (18) are the basic equations for this section. The solution is

$$\partial h_w/\partial t \begin{cases} -(H_w/\lambda)[C_1\exp(-L|\xi|/\lambda) \\ \quad +(\lambda\pi/L)(\beta_{11}\cos\pi\xi-\beta_{12}\sin\pi\xi)], & (\xi<0) \\ -(H_w/\lambda)[C_2\exp(-L|\xi|/\lambda) \\ \quad +(\lambda\pi/L)(\beta_{21}\cos\pi\xi-\beta_{22}\sin\pi\xi)], & (\xi>0) \end{cases} \tag{39}$$

where the parameters are defined by

$$\lambda = (g^*H_w)^{1/2}/f,$$

$$\beta_{11} = \pi C_{aw}u_i u_{a1}/f^2\lambda[1+(\lambda\pi/L)^2],$$

$$\beta_{12} = C_{aw}v_{a1}/f[1+(\lambda\pi/L)^2],$$

$$\beta_{21} = \pi C_{iw}u_i^2/f^2\lambda[1+(\lambda\pi/L)^2],$$

$$\beta_{22} = C_{iw}v_i/f[1+(\lambda\pi/L)^2],$$

$$C_1 = (\beta_{22}-\beta_{12})/2 + \lambda\pi(\beta_{21}-\beta_{11})/(2L)$$

$$C_2 = -(\beta_{22}-\beta_{12})/2 + \lambda\pi(\beta_{21}-\beta_{11})/(2L) \qquad (40)$$

where u_i, v_i are computed from nonhomogeneous linear algebraic equations (22a)-(22d). Eq.(39) shows that the ice breeze disturbance, which is local to the MIZ, will cause the reduced gravity ocean model to adjust to differential Ekman transport (both from changes in stress at the ice/ocean boundary and from horizontal variation in wind) by increasing or decreasing thickness. The rate of shallowing (thickening) is equivalent to an upwelling (downwelling). This effect of ice breeze on ice-edge upwelling/downwelling can be parameterized in terms of a differential surface heating condition, i.e.,

$$\partial h_w/\partial t = A_1 \exp(-L|\xi|/\lambda) + A_2[\partial\theta_a/\partial\xi - B(\theta_a-\theta_{a0})] \qquad (41)$$

where

$$A_1 = -(H_w C_1/\lambda)[1-H(\xi)] + (H_w C_2/\lambda)H(\xi),$$

$$A_2 = (H_w/LDT_0)\beta_{11}[1-H(\xi)] + \beta_{21}H(\xi), \qquad (42)$$

$$B = \pi(\beta_{12}/\beta_{11})[1-H(\xi)] + (\beta_{22}/\beta_{21})H(\xi).$$

Eq.(41) shows the relationship between ice-edge upwelling/downwelling and the surface temperature distribution across the ice edge.

We compute $\partial h_w/\partial t$ as a function of x and t for H_i=1, and 6m, respectively, as shown in Fig.8. It is seen that upwelling ($\partial h_w/\partial t < 0$) appears near the ice edge. The minimum value of $\partial h_w/\partial t$ (maximum upwelling) reaches 18.3 m day^{-1} for H_i = 1m, and 19.8 m day^{-1} for H_i=6 m. If the distance between two lines of -5 m day^{-1} is taken as the width of ice-edge upwelling, it is found that this width decreases with the increase of mean ice-thickness H_i. The upwelling width is around 40 km for H_i = 1m, and 25 km for H_i = 6m. These values are quite comparable to the baroclinic radius of deformation λ (23 km).

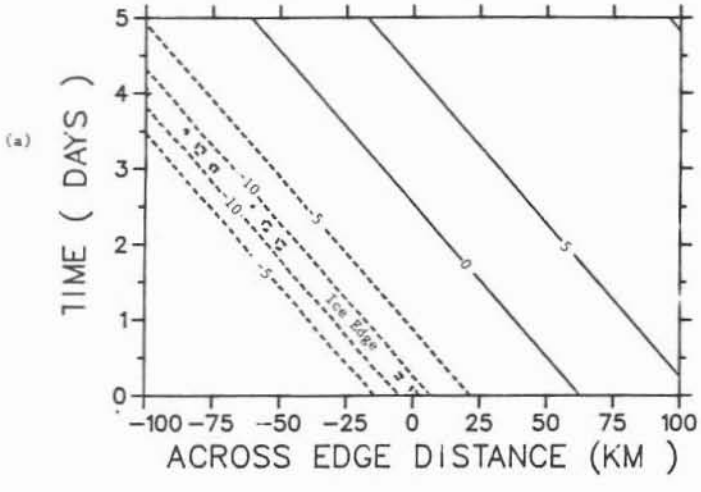

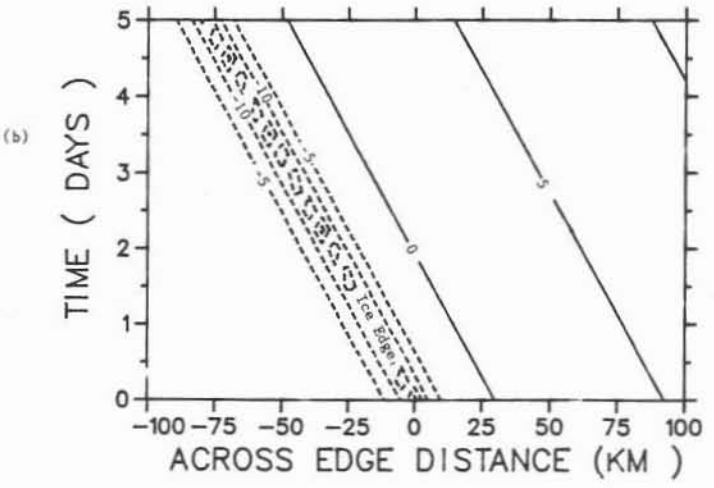

Fig.8. $\partial h_w/\partial t$ (m day^{-1}) as a function of x and t for (a) H_i = 1 m, and (b) H_i = 6 m.

CONCLUSIONS

(a) This air-ice-ocean coupled model is intended to depict only the mesoscale processes of air-ice-ocean interactions in the MIZ. The synoptic scale pressure gradient may additionally produce surface winds in the MIZ, and large-scale ocean current may also drive ice drift. These processes are, however, beyond the scope of this paper. Nevertheless, where the ice-to-open-water temperature gradient is strong, the mesoscale feedback mechanism discussed here may become as strong as, or stronger than, the synoptic scale and oceanic forcings.

(b) The model shows the different effects of ice breeze on ice flow, and gives out an ice divergence/convergence criterion in the MIZ.

(c) The ice motion has two bifurcations. First, it bifurcates into a decaying or growing mode, which depends in most cases on the mean surface temperature difference DT_0 representing the strength of the forcing. When DT_0 is small, the decaying mode exists. However, when DT_0 exceeds the first critical value, the growing mode appears. Secondly, the growing mode bifurcates into nonoscillatory and oscillatory states depending on DT_0 and the properties of ice.

(d) Surface winds, thermally generated by the temperature gradient across the ice edge, cause the reduced gravity ocean model to adjust to differential Ekman transport both from changes in stress at the ice/ocean boundary and from horizontal variation in winds. Such differential Ekman transport generates the ice edge upwelling.

ACKNOWLEDGEMENT

The author is grateful to Prof. H.L. Kuo of the University of Chicago and Prof. R.W. Garwood of the Naval Postgraduate School for invaluable discussion and comments. This research was supported by Grant OCE 85-15400 from the National Science Foundation, and the Research Foundation Fund from the Naval Postgraduate School.

REFERENCES

Buckley, J.R., T.Gammelsrod, J.A. Johannessen, O.M. Johannessen, and Roed, L.P., "Upwelling: oceanic structure at the edge of the Arctic ice pack in winter," *Science*, 203, 1979, 165-167.

Chu, P.C.,: "An instability theory of ice-air interaction for the migration of the marginal ice zone," *Geophys. J. R. Astr. Soc., 86, 1986a, 863-883.*

Chu, P.C., "An ice-air feedback mechanism for the migration of the marginal ice zone," *MIZEX Bull., VII, 1986b, 54-64.*

Chu, P.C., "A possible air-ice-ocean coupled model for the formation of leads or polynyas," *MIZEX Bull., VII, 1986c, 79-88.*

Chu, P.C.: "Generation of unstable modes of the iceward attenuating swell by ice breeze," *J. Phys. Oceanogr.* 1987a, 828-832.

Chu, P.C.: "An instability theory of ice-air interaction for the formation of ice edge bands," *J. Geophys. Res., 1987b,* 6966-6970.

Chu, P.C.: "An icebreeze mechanism for an ice divergence-convergence criterion in the marginal ice zone," *J. Phys. Oceanogr., 1987c,* 1627-1632.

Chu, P.C.: "An air-sea feedback mechanism for quasi-geostrophic water movement near a fast shelf-ice edge with a small curvature," *Chinese J. Atmos. Sci.*, Allerton Press, New York, 1987d, 31-42.

Gill, A.E.: *Atmosphere-Ocean Dynamics* Academic Press, New York, 1982, p466.

Hibler, W.D.III., and Ackley S.F., "Numerical simulation of the Weddell Sea pack ice," *J. Geophys. Res.*, 88, 1983, 2873-2887.

Kuo, H.L., "Planetary boundary layer flow of a stable atmosphere over the globe," *J. Atmos. Sci.*, 30, 1973, 53-65.

Lepparanta, M. and Hibler, W.D., "On the role of plastic ice interaction in marginal ice zone dynamics," *J. Geophys. Res., 90, 1985,* 11899-11909.

McPhee, M.G., "Turbulent heat and momentum transfer in the oceanic boundary layer under melting pack ice," *J. Geophys. Res.*, 88, 1983, 2827-2835.

Muench, R.D., "Mesoscale oceanographic features associated with the central Bering Sea ice edge: February-March 1981," *J. Geophys. Res., 88, 1983,* 2715-2722.

Muench, R.D., and Schumacher, J.D., "On the Bering Sea ice edge front," *J. Geophys. Res.*, 90, 1985, 3185-3197.

Paquette, R.G., and Bourke, R.H., "Temperature fine structure near the sea-ice margin of the Chukchi Sea," *J. Geophys. Res., 84, 1979, 1155-1164.*

Reynolds, M., C.H. Pease, and Overland, J.E., "Ice drift and regional meteorology in the southern Bering Sea: results from MIZEX West," *J. Geophys. Res., 90, 1985,* 11967-11981.

Roed, L.P., and O'Brien, J.J., "A coupled ice-ocean model of upwelling in the marginal ice zone," *J. Geophys. Res.*, 88, 1983, 2863-2872.

Schmidt, F.H., "An elementary theory of the land- and sea- breeze circulation," *J. Meteor.*, 4, 1947, 9-15.

Vinje, T.E., "The drift pattern of sea ice in the Arctic with particular reference to the Atlantic approach," *The Arctic Ocean*, Wiley, New York, 1982, 83-96.